Effects of both Grain and Grain Boundary Strengths on the Creep Rupture Strength of Austenitic Heat Resisting Steels

Mitsuyuki KOBAYASHI*

(Received October 31, 1973)

1. Introduction

Metals and alloys for engineering service are in general polycrystalline aggregates. However, at room temperature since the slip planes are generally weaker than the grain boundaries, the strength is determined only by the grain strength. On the other hand, the strength at elevated temperature, especially creep rupture strength, becomes very dependent on both grain and grain boundary strengths because the grain boundary strength decreases more rapidly than the grain strength as temperature increases. In this respect, the effect of grain strength on the creep rupture has been already reported[1)~4)], showing the relationship between creep rupture time t_r and minimum creep rate $\dot{\varepsilon}_m$, or $t_r \propto \dot{\varepsilon}_m^{-1}$. This relationship indicates that the strengthening of grains contributes to the increase in the creep rupture strengh since $\dot{\varepsilon}_m$ decreases with the strength since $\dot{\varepsilon}_m$ decreases with the strength of grains. Several papers[5)~9)] have also shown that the creep rupture strength was increased by the strengthening of grain boundaries due to irregular coarse precipitates formed on them. In these studies, however, the combined effect of these two strengths on the creep rupture strength was not apparent.

This paper presents the effects of both grain and grain boundary strengths on the creep rupture strength of austenitic heat resisting steels and shows the effective methods to improve the creep rupture strength by strengthening both grains and grain boundaries, respectively.

2. Materials and Experimental Procedures

Chemical compositions of specimens used in this experiment are shown in Table 1. 21–12 N and CRK 22 steels are both austenitic heat resisting steels and can also be age-hardend by $M_{23}C_6$ carbides. Both steels were solution-treated at 1200°C for 1 hr so that age hardening components could be in complete solution in matrix. To obtain a wide range of grain strengths, aging treatment condi-

* Lecturer, Department of Mechanical Engineering

Table 1. Chemical compositions of specimens (wt. %)

Steel	C	Si	Mn	P	Ni	Cr	Mo	N	Others	Fe
CRK22	0.31	0.37	0.96	0.20	10.51	19.55	1.98	—	Cu 0.7 B 0.005	bal.
21-12N	0.19	0.72	1.16	0.03	10.42	21.72	—	0.23	—	bal.

tions were changed, in particular to 21-12N steel cold working was added before aging treatment. Furthermore different cooling procedures from solution temperature were employed to give various grain boundary strengths to specimens.

Hardness was measured at room temperature by Akashi Vickers hardness tester, and the creep rupture test was carried out at 700°C with Tohshin spring type multi creep rupture tester. The size of the creep rupture specimen was $6\phi \times 30$ G. L.

Specimens for metallographic examination were finally polished with most fine gamma alumina powder. The etchant was a mixture of HNO_3, HCl and glycerine with mixing ratio of 1:2:2 by volume. The observation of microstructures was mainly carried out with a optical microscope.

3. Experimental Results

3.1 Grain and grain boundary strengths of specimens

It was experimentally shown[10)11)] that the grain strength or 0.2 percent proof stress was proportional to the hardness at room temperature, and so at

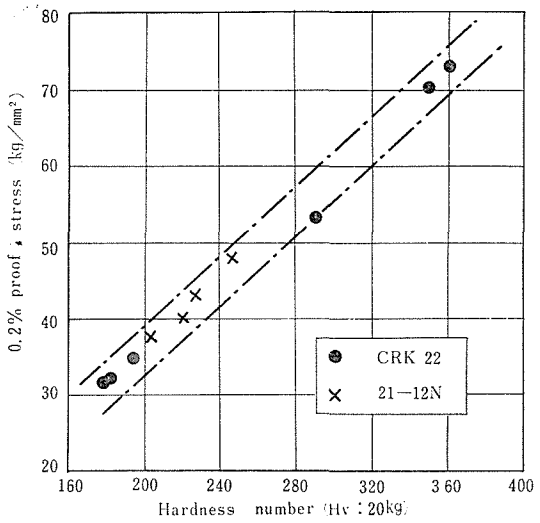

Fig. 1 Relationship between 0.2% proof stress and hardness at room temperature.

elevated temperatures. Therefore it is apparent that relative grain strengths at high temperatures can be fully expressed by the hardness at room temperature. Fig. 1 shows the relation between 0.2 percent proof stress and Vickers hardness of 21–12N and CRK22 steels obtained in this experiment.

For grain boundary strengths, it has already been reported[5)~9)] that variation in grain boundary strength was attained by various cooling procedures. It was found that irregular coarse precipitates formed on grain boundaries during slow cooling from solution temperatures resulted in the strengthening of grain boundaries, and that the more and the coarser the precipitates are, the stronger the grain boundaries become. In this investigation too, similar procedures for obtaining various grain boundary strengths, namely water quenching, air cooling, and furnace cooling were used, especially to CRK22 steel two step cooling procedure was added. This procedure is to quench specimens to room temperature after furnace cooling from solution temperature to a relatively high temperature range, by which the same level of the grain boundary strength as furnace cooling can be reached.

From the results obtained by the observation of microstructures, the grain boundary strengths σ_{gb} of the specimens cooled various procedures were relatively given by in 21–12N,

$$(\sigma_{gb})_{WQ} \approx (\sigma_{gb})_{AC} < (\sigma_{gb})_{FC}, \tag{1}$$

where *WQ*, *AC* and *FC* indicate water quenching, air cooling and furnace cooling, respectively. In CRK22 steel, however, even air cooling produced partly irregular and coarse precipitates, so the order of grain boundary strengths became

$$(\sigma_{gb})_{WQ} < (\sigma_{gb})_{AC} < (\sigma_{gb})_{FC} \approx (\sigma_{gb})_{FQ}, \tag{2}$$

where *FQ* indicates two step cooling procedure. It is considered that the grain boundary strength increases with increasing surface energy of a crack formed on the boundaries, γ, because initiation and propagation of the crack are so suppressed as γ becomes higher. Therefore it is supposed that γ can be used as a measure of σ_{gb}. Then the following expressions hold from (1) and (2).

$$\gamma_{WQ} \approx \gamma_{AC} < \gamma_{FC}, \qquad \text{in 21–12N} \tag{3}$$

$$\gamma_{WQ} < \gamma_{AC} < \gamma_{FC} \approx \gamma_{FQ}. \qquad \text{in CRK22} \tag{4}$$

On the basis of above considerations, solution treatments followed by various cooling procedures and aging treatments were performed for obtaining various grain and grain boundary strengths, and hardness was measured at room tem-

Table 2. Hardness values after various heat treatments

Steel	Heat treatment*	Hardness (Hv: 20kg)
21–12N	1200°C×1hr →WQ+600°C×100hr →AC	263
	1200°C×1hr →WQ+800°C× 3hr →AC	229
	1200°C×1hr →AC	221
CRK22	1200°C×1hr →WQ+600°C× 100hr →AC	380
	1200°C×1hr →WQ+800°C× 1hr →AC	345
	1200°C×1hr →WQ+900°C× 1hr →AC	329
	1200°C×1hr →WQ+1000°C× 1hr →AC	288
	1200°C×1hr →AC+600°C× 100hr →AC	382
	1200°C×1hr →AC+800°C× 1hr →AC	349
	1200°C×1hr →AC+900°C× 1hr →AC	320
	1200°C×1hr →AC+1000°C× 1hr →AC	293
	1200°C×1hr →FC+600°C× 200hr →AC	308
	1200°C×1hr →FC+700°C× 30hr →AC	278
	1200°C×1hr →FC+850°C× 5hr →AC	260
	1200°C×1hr →FC+900°C× 3hr →AC	247
	1200°C×1hr →FC+1000°C× 3hr →AC	242

* Heat treatments shown above include the final aging treatment of 750° C, 100hr.

Table 3. Aged hardness of cold-worked specimens of 21–12N steel.

Cooling procedure	Extent of cold working in tension (%)	Aging time (hr) 0	3	10	30	100	300
Water-quenched	2	226	229	244	263	260	262
	5	250	257	274	280	273	277
	10	280	280	302	295	292	291
	20	326	332	325	323	312	315
Furnace-cooled	2	220	217	221	230	233	237
	5	240	235	241	253	250	254
	10	277	264	270	285	273	271
	20	320	300	302	302	292	297

Solution treatment : 1200°C×1hr (Hv: 20kg)

perature. The results are shown in Table 2. Since the same hardness level as water-quenched could not be obtained in furnace-cooled specimens of 21–12N steel, the specimens were cold-worked after solution treatment and aged. The results are shown in Table 3, which indicated that the hardness of furnace-cooled specimens approached nearly to that of water-quenched.

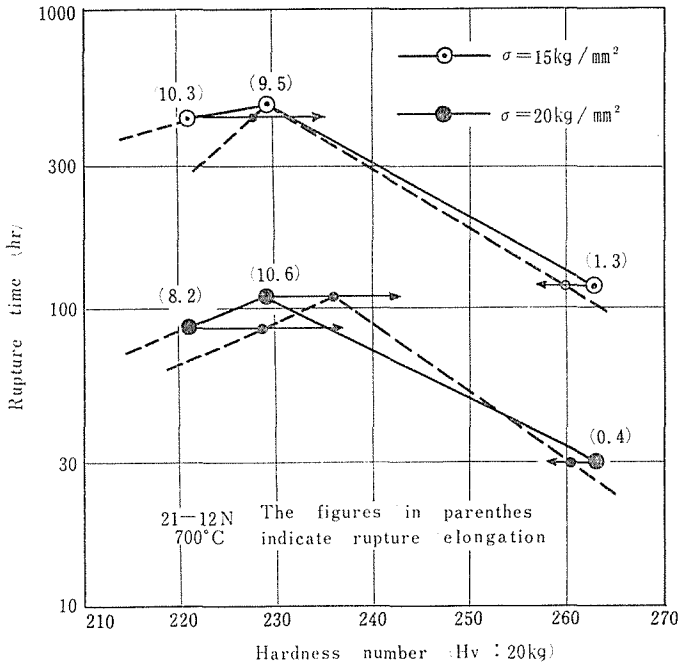

Fig. 2 Effect of grain strength on the creep rupture time.

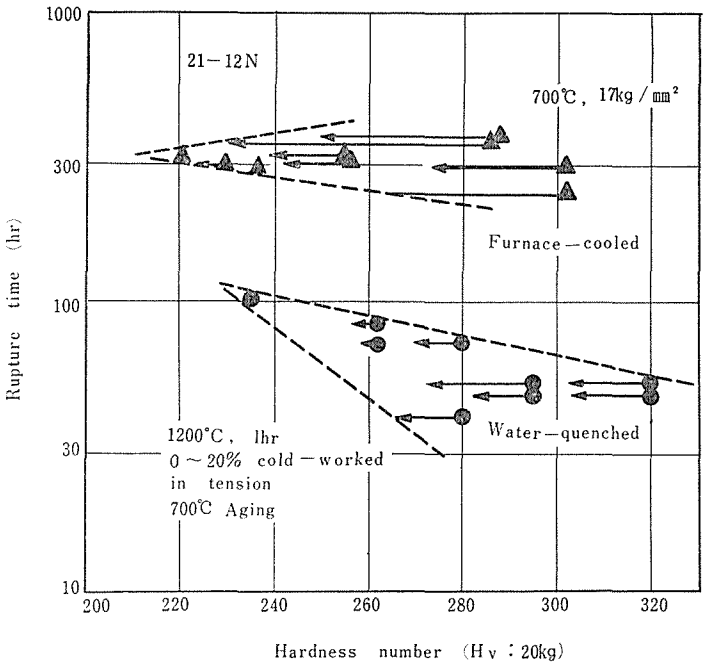

Fig. 3 Effects of grain and grain boundary strengths on the creep rupture time.

Table 4. Creep rupture time tested at 700°C, 17kg/mm² of 21–12N steel

Cooling procedure	Number of specimen	Extent of cold working in tension (%)	Rupture time (hr)	Rupture elongation (%)	Hardness (Hv:20kg)	
					Before test	After test
Water-quenched*	10	1.9	83.0	0.34	262	257
	12	1.9	70.3	0.48	262	260
	16	5.2	40.0	0.55	280	265
	17	5.1	72.5	0.18	280	270
	4	11.0	49.0	0.20	295	282
	5	11.1	52.0	0.27	295	272
	22	19.7	52.0	0.26	320	305
	23	19.9	47.0	0.19	320	306
	N20	0.0	102.0	4.55	234	238
Furnace-cooled*	8	2.7	288.5	3.18	236	238
	9	1.8	292.0	3.15	229	223
	13	5.3	301.5	2.23	256	242
	14	5.3	308.0	2.42	256	239
	2	10.8	351.0	1.79	286	230
	3	10.0	367.0	0.44	285	250
	20	20.1	243.5	0.94	302	264
	21	20.2	290.0	0.73	303	273
	N26	0.0	320.0	12.77	202	218

* All specimens were solution-heated and cold-worked followed by aging of 700°C, 30hr before rupture test

On these specimens the creep rupture test was carried out at 700°C.

3.2 Creep rupture test of 21–12N steel

Effect of grain strength on the creep rupture time fo 21–12N steel are shown in Fig. 2. Since specimens used were heat-treated as shown in Table 2, these grain boundary strengths are almost equal. Each point in this figure indicates the relationship between the hardness before test and the creep rupture time, and the head of arrows shows the hardness after test. Therefore the solid line shows the relation between the hardness before test and the creep rupture time, the dotted line showing the case of the mean hardness before and after tests. However any distinct difference could not be found between both relationships. Then it can be said from Fig. 2 that the increase in the grain strength can not always lead to the increase in the creep rupture strength. But it is likely that the data of the test is not sufficient to determine the quantitative relationship between the grain strength and the creep rupture time.

Table 4 and Fig. 3 show the results of 700°C creep rupture test of specimens

cold-worked after solution treatment followed by aging of 700 °C, 30hr. The stress was 17kg/mm². The remarkable effect of grain boundary strengths is seen in Fig. 3, while the effect of grain strengths was not well known since change in hardness during test was quite large.

3.3 Creep rupture test of CRK22 steel

The results of creep rupture test at 700°C, 30kg/mm² are shown in Fig. 4. The specimens were heat-treated as indicated in Table 2. In addition, two step cooling procedure was employed to give specimens, which have the same grain boundary strength as furnace-cooled specimens, the aged hardness of about Hv 350. The arrows show the same as in 21-12N steel.

The most characteristic point in this figure was that the effect of grain boundary strength did not appear at lower hardness, but the remarkable effect yielded at higher hardness region. Further, the rupture time of water-quenched specimens increased linearly to the hardness of Hv 310, but decreased with hardness over Hv 310. For air-cooled specimens, the rupture time increased

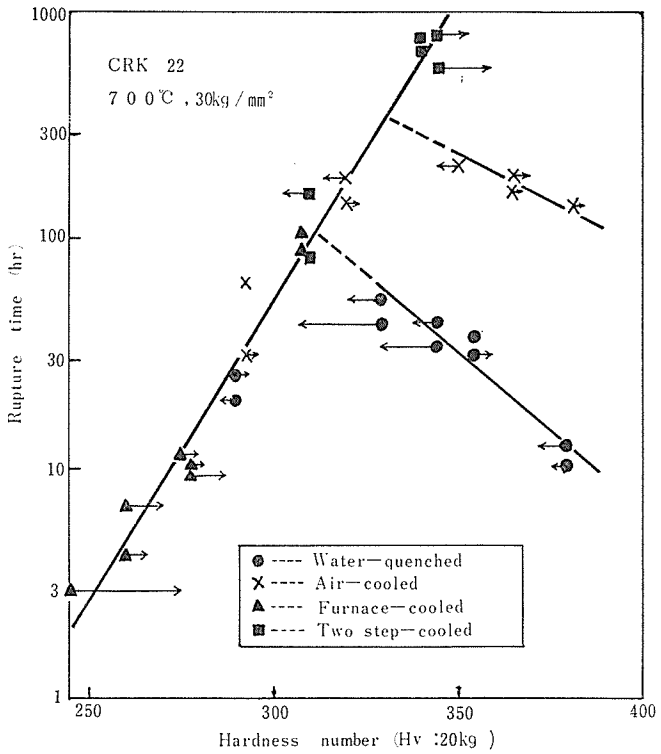

Fig. 4 Effects of grain and grain boundary strengths on the creep rupture time.

also to around Hv 330, but there was a gradual decrease in the rupture time over Hv 330. The linear relationship of the rupture time and the hardness under the conditions employed here only existed in furnace-cooled, and two step-cooled specimens, which had the strongest grain boundary strength. If the hardness higher than Hv 350 were obtained in two step-cooled specimens, the same tendency as in the water-quenched or the air-cooled specimens would appeared there.

It is therefore said that the hardness at which the rupture time begins to decrease becomes higher as the grain boundary strength increases. Since large changes in hardness and grain boundary strength were not found during the test, the following relationship between creep rupture time and hardness can be introduced from Fig. 4. Namely, for the ascending portion of the curve,

$$\log t_r = b + aH_v \tag{5}$$

is introduced, where a and b are constants. And for the descending portion,

$$\log t_r = B - AH_v \tag{6}$$

holds where A and B are variables of grain boundary strength.

Fig. 5 indicates the creep rupture elongation. In all specimens the elongations decreased rapidly with hardness and the value of 2 percent began to prevail at the same hardness region as that for the rupture time to start decreasing.

3.4 Type of cracks found in ruptured specimens

W-type cracks were found in specimens ruptured within 100 hr, and R-type cracks began to exist in specimens ruptured at around 300 hr and were dominant at further pro-longed life. Therefore it can be said that the creep rupture is caused by W-type cracks at short life within 100 hr, and by R-type cracks at long life over 300 hr. An example of these cracks is shown in Photo. 1.

4. Discussion

It will be assumed that creep rupture strength or time could be accurately calculated if the machanisms of both initiation and propagation of W-type crack or R-type crack were known. At present, however, these mechanisms are not explained completely. Therefore detalied discussions on creep and creep rupture are avoided. The discussion here is aimed mainly to clarify the effects of grain and grain boundary strengths on the creep rupture time from the standpoint that the creep rupture strength are determined by these two strengths.

4.1 Creep rupture mechanism

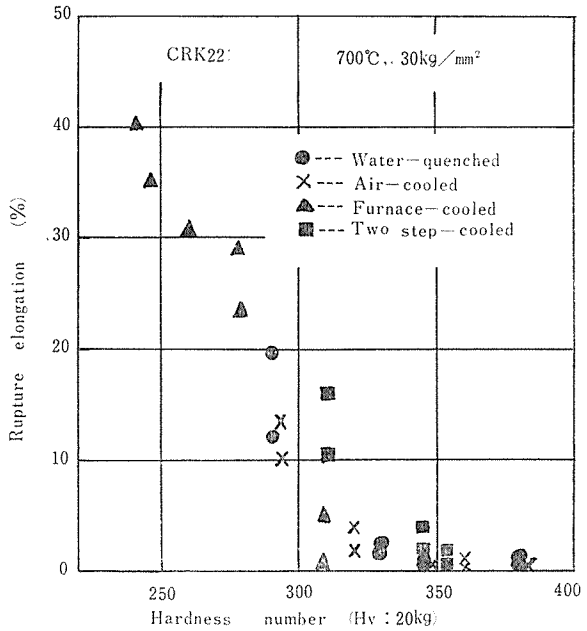

Fig. 5 Relationship between hardness and rupture elongation.

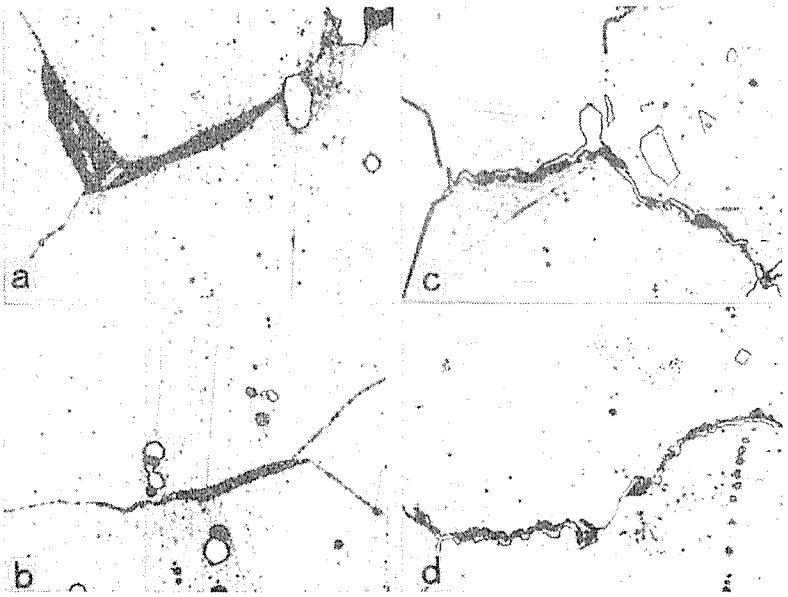

(a) and (b) Water-quenched specimen ruptured at 33hr, showing W-type cracks.
(c) and (d) Two step-cooled specimen ruptured at 760 hr, showing R-type cracks.

Photo. 1 Microstructures of ruptured specimens.

It can be concluded from the experimental results that the relation, $\log t_r = b + aH_v$, is always maintained if the grain boundary strength increases adequately in comparison to the increase in the grain strength. This fact suggests that specimens satisfied the above relation all ruptured by the same mechanism regardless of grain boundary strengths. On the other hand, it is also considered that quite another mechanism operates in the specimens satisfied the relationship, $\log t_r = B - AH_v$. It is discussed here on these mechanisms.

4.1.1 Mechanism operating for the relationship of $\log t_r = b + aH_v$

The linear relationship shown in Fig. 4 was held from several hours to around 800 hr. Cracks at grain boundaries observed were W-type at shorter life and R-type at longer life. At intermediate life both types were found. These cracks found in one specmen were large in number. This fact indicates that the time to rupture is controlled by the growth rather than the nucleation of cracks and that the growth mechanism is the same in both types. Therefore the nucleation of cracks are not discussed from now.

Many investigations have been carried out on the growth mechanisms of W-type and R-type cracks. Zener[12] proposed at first that the nucleation and the growth of a W-type crack was caused by grain boundary sliding. After that, the creep rupture mechanism and the rupture life were studied[13][14] on the basis of Zener mechanism. It can therefore be assumed that the growth of W-type crack is due to grain boundary sliding.

Two essentially different views have been proposed to describe the growth of R-type cracks. The diffusion growth models[15][16] consider the crack to be fed by a flux of vacancies generated in the grain boundary by the applied tensile stress; the other view[17][18] is the deformation growth model. This assumes that the cavity behaves as a shear crack, which grows by grain boundary sliding. Both viewpoints owe thier viability to certain key experiments[19]~[21] which appear to support one mechanism and exclude the other.

Recently, however, Evans[22] proposed the new idea supporting the deformation growth model and explained successfully the experimental results which could not be explained by the old deformation growth model.

In view of the studies mentioned above, and the results obtained in this experiment, it is proper to conclude that both W-type and R-type cracks grow by grain boundary sliding and that the rupture in the region shown by the relation $\log t_r = b + aH_v$ occurs by the growth of W-type cracks or R-type cracks.

4.1.2 Mechanism operating for the relationship of $\log t_r = B - AH_v$

In this region all specimens tested ruptured by W-type cracks, which were

scarcely observed near the ruptured parts. In addition, the rupture elongation were all very low as described previously. Therefore it can be assumed that cracks nucleated at the grain boundary propagated rapidly to rupture. In conclusion, the creep rupture may controlled by the initiation of a W-type crack.

4.2 Estimation of rupture time

4.2.1 Expression for rupture time controlled by the growth of a crack

Langdon[12] introduced the following expression of the rupture time applying Cottrell's equation[23] on the equilibrium length of the crack at brittle fracture to a crack produced by creep.

$$t_r \approx \left\{\frac{8\pi(1-\nu)\gamma(2C_{fr})}{G}\right\}^{\frac{1}{2}} \cdot \frac{1}{D} \cdot \frac{1}{\dot{\varepsilon}_{gb}}, \tag{7}$$

where ν, G, $\dot{\varepsilon}_{gb}$, C_{fr}, D and γ are Poisson's ratio, modulus of rigidity, rate of grain boundary sliding, crack length at fracture, grain diameter and surface energy of crack, respectively. On the other hand, the expression for the rupture time caused by R-type cracks grown due to grain boundary sliding has not yet been proposed. Only the relation between the rate of grain boundary sliding and the growth rate of R-type cracks were found by Evans.[22] That is,

$$\frac{dl}{dt} = \left\{1 - \frac{\pi(1-\nu)}{8G\gamma}\sigma_n{}^2 l - \frac{\sigma_n h}{2\gamma}\right\}^{-1} D\dot{\varepsilon}_{gb}, \tag{8}$$

where l, σ_n and h are crack length measured to the direction of grain boundary sliding, normal stress and thickness of crack, respectively. For simplicity, assuming that the thickness h is very small relative to the length l, that is, $h/l \approx 0$, the unstable crack length was expressed by $l = 8G\gamma/\pi(1-\nu)\sigma_n{}^2$ [22]. Here the assumption that the rupture would occur when the crack length reaches to the unstable crack length is made. Then the expression of the rupture time is given from Eq. (8).

$$t_r \approx \frac{4G\gamma}{\pi(1-\nu)\sigma_n{}^2} \cdot \frac{1}{D} \cdot \frac{1}{\dot{\varepsilon}_{gb}}. \tag{9}$$

Eqs. (7) and (9) are for the rupture time determined by the growth of W-type and R-type cracks, respectively. Since the rate of grain boundary sliding is nearly proportional to the minimum creep rate[2,25], $\dot{\varepsilon}_{gb}$ is given by,

$$\dot{\varepsilon}_{gb} \approx \alpha\dot{\varepsilon}_m, \tag{10}$$

where α is constant. It is apparent that $\dot{\varepsilon}_m$ is the factor associated with grain strength. Therefore the following equations are obtained, expressing only in

terms of γ, $\dot{\varepsilon}_m$ and constants.

$$\text{For W-type crack} \qquad t_r \approx K_W \gamma^{\frac{1}{2}} \dot{\varepsilon}_m^{-1}. \tag{11}$$

$$\text{For R-type crack} \qquad t_r \approx K_R \gamma \dot{\varepsilon}_m^{-1}. \tag{12}$$

Next the relationship between $\dot{\varepsilon}_m$ and proof stress σ_p must be obtained. Cottrell[25] proposed that creep strain rate $\dot{\varepsilon}$ is given by

$$\dot{\varepsilon} = C \exp\left\{-\frac{V(\sigma_o - \sigma)^n}{\kappa T}\right\}, \tag{13}$$

where κ and T are Boltzmann's constant and absolute temperature, and C, σ_o, V are constants. In this equation it was reported that n equals unity when dislocations moves through the particles distributed uniformly in matrix[24]. In this investigation too, the conditions are considered to be similar to that described above because specimens were all age-hardened by precipitates formed at random in matrix. Then in Eq. (13) the term $V\sigma_o$ is the activation energy which dislocations must overcome. When tensile test is carried out at room temperature where the effect of heat perturbation is negligibly small, the stress for the specimens to deform plastically must at first be applied so that dislocations can overcome the barrier of the activation energy $V\sigma_o$. Namely the plastic deformation occurs when the applied stress σ reaches to the value which satisfies

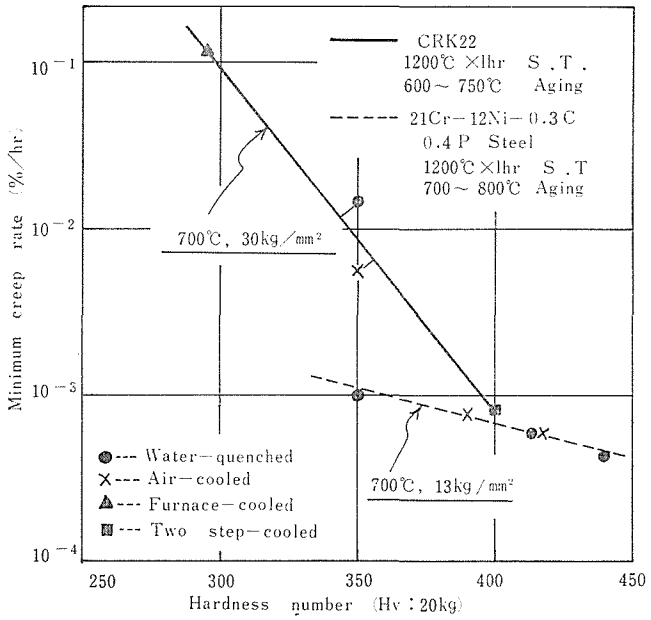

Fig. 6 Relationship between hardness and minimum creep rate.

$V(\sigma_o - \sigma) = 0$. Then this stress is apparently the proof stress σ_p of specimens, that is, $\sigma_p = \sigma_o$. And replacing $\dot{\varepsilon}$ by $\dot{\varepsilon}_m$ gives

$$\dot{\varepsilon}_m = C \exp\left\{-\frac{V(\sigma_o - \sigma)}{\kappa T}\right\}. \tag{14}$$

Substituting $\sigma_p = b_o + a_o H_v$ into Eq. (14),

$$\dot{\varepsilon}_m = C' \exp\left\{-\frac{V(a_o H_v - \sigma)}{\kappa T}\right\} \tag{15}$$

is obtained. The above relationship was in good agreement with the experimental data shown in Fig. 6 which could be obtained in CRK22 and 21Cr-12Ni-0.3C-0.4N steels[26]. Substituting Eq. (15) into Eqs. (11) and (12), and assuming σ and T are constants, the following equations can be obtained.

For W-type crack $\quad t_r \approx K_W \gamma^{\frac{1}{2}} e^{\beta H v}$. (16)

For R-type crack $\quad t_r \approx K_R \gamma e^{\beta H v}$. (17)

Eqs. (16) and (17) are found to be the same as Eq. (1).

4.2.2 Expression for rupture time controlled by the nucleation of a crack

Yokobori[27] proposed that the rupture time can be expressed in terms of the probability of the nucleation of a crack, m, when the rupture is determined by the nucleation of a crack as in glass. The probability m and the rupture time are given by,

$$m = A_o T \exp\left(-\frac{\Delta F}{\kappa T}\right) \sinh\left(\frac{B_o \sigma}{\kappa T}\right), \tag{18}$$

$$t_r = 1/m$$

$$= \frac{1}{A_o T} \exp\left(\frac{\Delta F}{\kappa T}\right) \sinh\left(-\frac{B_o \sigma}{\kappa T}\right), \tag{19}$$

where ΔF and σ are the activation energy for the nucleation of a crack and applied stress. And A_o, B_o are constants. Since $B_o\sigma/\kappa T \gg 1$ under the usual testing conditions, Eq. (19) becomes approximately,

$$t_r = \frac{1}{A_o T} \exp\left(\frac{\Delta F - B_o \sigma}{\kappa T}\right). \tag{20}$$

Assuming that ΔF is nearly proportional to γ,

$$\Delta F \approx \alpha_o \gamma \tag{21}$$

is obtained where α_o is constant.

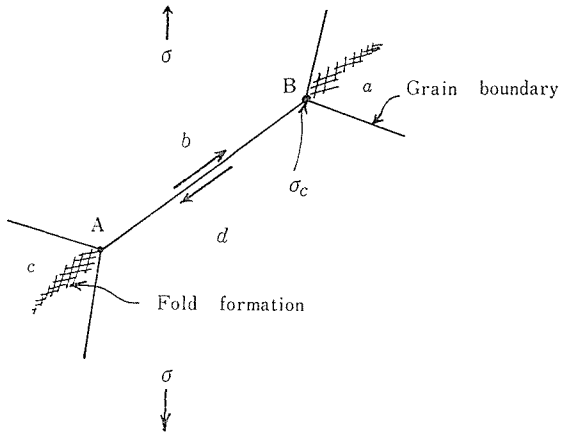

Fig. 7 Stress concentration at tripple points due to grain boundary sliding.

It will be considered next on the relation between Eq. (20) and grain strength or proof stress. Here grains a, b, c and d which have the proof stress of σ_p are taken as illustrated in Fig. 7. Further it is supposed here for simplicity that grain boundary sliding occurs only along the grain boundary AB. Then the stress σ_c at the tripple point A or B is increased by the stress concentration when grain boundary sliding occurs. The stress σ_c are relieved by the local plastic deformation or the fold formation in the grain a or c. Therefore the stress concentration increases with the increase in the proof stress of grains. Consequently, it is considered that the extent of the stress concentration at the tripple point is proportional to the proof stress of the specimen. Namely, the stress concentration factor q is given by,

$$q = \sigma_c/\sigma = q_1\sigma_p,$$

and hence

$$\sigma_c = q_1\sigma_p\ \sigma, \tag{22}$$

where q_1 is constant. Since the nucleation of a crack is determined by the stress σ_c, σ in Eq. (20) is considered to be σ_c. Then substituting Eqs. (21) and (22) into Eq. (20), the rupture time is given by,

$$t_r \approx \frac{1}{A_0 T} \exp\left(\frac{\alpha_0\gamma - B_0 q_1 \sigma_p \sigma}{\kappa T}\right).$$

In view of $\sigma_p = b_0 + a_0 H_v$ and supposing T and σ are constants, the rupture time becomes

$$t_r \approx K_I e^{(\alpha_0\gamma - \beta_0 H_v)}, \tag{23}$$

where K_I, α_o and β_o are constants.

The above expression of t_r is the same as Eq. (2) obtained by the experimental data.

4.3 Effects of the strengths of grains and grain boudaries on the creep rupture time

To clarify effects of these factors on the creep rupture time, Eqs. (16), (17) and (23) are expressed by logarithm as follows.

$$\log t_r \approx \log K_W + \frac{1}{2} \log \gamma + \beta H_v, \tag{24}$$

$$\log t_r \approx \log K_R + \log \gamma + \beta H_v, \tag{25}$$

$$\log t_r \approx \log K_I + \alpha_o \gamma - \beta_o H_v. \tag{26}$$

From Eqs. (24) and (25) it is apparent that the effects of γ, K_W and K_R are far smaller than that of Hv since γ, K_W and K_R are expressed by logarithm. Therefore Eqs. (24) and (25) can be combined to the following equation.

$$\log t_r \approx \log K_c + A_c \log \gamma + \beta H_v. \tag{27}$$

On the other hand, from Eq. (26) it is recognized that these two factors are both important under the condition where the rupture time is determined by the nucleation of a crack. This explaines well the results for the descending portion of curves shown in Fig. 4.

The relationship between Hv and γ where the peak rupture time appears can be obtained by putting the right hand side of Eq. (26) equal to that of Eq. (27), that is,

$$\log K_I + \alpha_o \gamma - \beta_o H_v = \log K_c + A_c \log \gamma + \beta H_v.$$

Neglecting $\log \gamma$ since $\gamma \gg \log \gamma$, then

$$\gamma \approx \frac{1}{\alpha_o}\{(\beta + \beta_o) H_v + \log (K_c/K_I)\} \tag{28}$$

is obtained. Fig. 8 shows qualitatively the relationship between t_r, Hv and γ obtained from Eqs. (26) and (27). Then H_v-γ plane can be divided into two regions by the line ll' which expresses Eq. (28).

Here A is the region where Eq. (27) holds; the growth of cracks determines the rupture and the effect of the grain strength on the rupture strength is far greater than that of the grain boundary strength. On the contrary, B is the region where Eq. (26) can be applied; the nucleation of a crack determines the rupture and the strengthening of the grain boundary contributes very much to

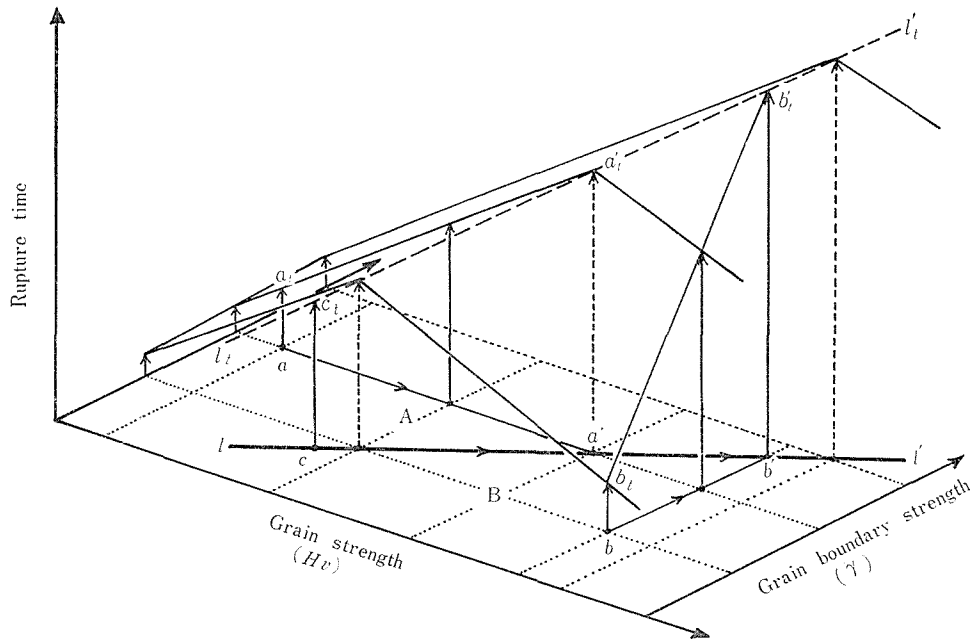

Fig. 8 Schematic representation of the effects of both grain and grain boundary strengths on the creep rupture time.

the improvement in the rupture strength and that the increase in the grain strength results in the decrease in the rupture strength.

Now the strengths of grain and grain boundary of alloys are supposed to be given as point a, b or c as shown in Fig. 8. At first the alloy given by point a is considered. The improvement in the creep rupture strength is achieved as described following : the grain strength must be increased to a'. Then the rupture time increases from a_t to a_t'. Next both the grain and the grain boundary can be strengthened at the same time along the line ll'. The alloy shown by point b is next taken. The creep rupture strength may be increased by the following procedures : firstly the grain boundary strength must be increased to b'. This leads to the increase in the rupture time from b_t to b_t'. Secondary, both strengths must be increased along ll'. For the improvement in the rupture strength of the alloy given by point c, it is desired that the grain and the grain boundary are both strengthened along ll' from the first.

5. Conclusions

In the present paper, the effects of both strengths of grains and grain boundaries on the creep rupture time of 21-12N, and CRK22 steels were inves-

tigated. The results obtained are summarized as follows:

1) With 21-12N steel the effects of both stregths on the time to rupture could not be found, since various specimens which have a wide range of hardness could not be obtained and great variations in grain strength or hardness took place during test at 700°C.

2) On the other hand, in CRK22 steel the distinct effects of these strengths on the creep rupture time could be obtained because of no change in hardness during test. Therefore the experimental expressions for the time to rupture were given by $\log t_r = b + aH_v$ for lower hardness region, where a and b are constants. And for higher hardness region, $\log t_r = B - AH_v$, where A and B are variables of the grain boundary strength.

3) The expression for lower hardness region can be obtained on the assumption that the creep rupture ascribes to the growth of cracks due to grain boundary sliding and that the proof stress is proportional to the activation energy of creep. That for higher hardness region can also be obtained on the assumption that the nucleation of a crack determines the rupture of specimens and that the stress concentration at a tripple point of grain boundary increases proportionally with the proof stress.

4) After all when specimens possess sufficient grain boundary strength, the increase in grain strength leads straightly to the improvement in the rupture strength. On the contrary, when the strength of grain boundaries is relatively lower than grains, the strengthening of grain boundaries has a marked effect on the improvement in the rupture strength, which is inclined to decrease with the increase in grain strength. In order to improve the creep rupture strength, therefore, it is desirable firstly to investigate fully the relationship between both strengths.

ACKNOWLEDGEMENTS

Gratitude is extended to Prof. O. Miyagawa, M. Yamamoto, Y. Mochiki and Y. Inoue in Tokyo Metropolitan University without whose assistance and cooperation this work would not have been possible.

References

1) F. Garofalo, R. W. Whitemore et al: Trans. AIME, **221** (1961), 310.
2) I. S. Servi and N. J. Grant: Trans. AIME, **191** (1951), 909.
3) F. C. Monkman and N. J. Grant:Proc. ASTM, **56**(1956), 834.
4) P. Feltham and J. D. Meakin : Acta Met., **7**(1959), 614.
5) W. Betteridge and A. W. Franklin : J. Inst. Metals, **85**(1956-57), 473.
6) C. W. Weaver: J. Inst. Metals, **88**(1959-60), 462.

7) M. Yamazaki: Trans JIM, **9**, (1968), 162 (Proceedings of the International Conference on the Strength of Metals and Alloys, Tokyo).
8) T. Saga, O. Miyagawa, M. Kobayashi and D. Fujishiro : Trans. ISIJ, **11** (1971), 157.
9) M. Kobayashi, M. Yamamoto, O. Miyagawa, T. Saga, and D. Fujishiro : Tetsu-to-Hagane, **58**(1972), 859.
10) Japan Institute of Metals:Metals Handbook, (1971), 437, Maruzen.
11) J. R. Mihalisin and R. F. Decker : Trans, AIME, **218**(1960), 507.
12) C. Zener : Elasticity and Anelasticity of Metals, (1948), University of Chicago Press.
13) J. A. Williams : Acta Met., **15**(1967), 1559.
14) T. G. Langdon : Phil. Mag., **22**(1970), 945.
15) R. W. Balluffi and L. L. Seigle : Acta Met., **3**(1957), 449.
16) D. Hull and D. E. Rimmer : Phil. Mag., **4**(1959), 673.
17) R. C. Gifkins: Acta Met., 4(1956), 98.
18) C. W. Chen and E. S. Mashilin : Acta Met., **4**(1956), 655.
19) R. T. Ratcliffe and G. W. Greenwood : Phil. Mag,. **12**(1965), 59.
20) P. W. Davis and R. Dutton : Acta Met., **14**(1966), 1138.
21) P. W. Davis and K. R. Williams : Met. Sci. J., **3**(1969), 220.
22) H. E. Evans : Phil. Mag., **23**(1971), 1101.
23) A. H. Cottrell : Trans. AIME, **212**(1958), 192.
24) F. Garofalo : Fundamentals of Creep and Creep Rupture in Metals (1968), 141, Maruzen (translated by M. Adachi).
25) A. H. Cottrell : Structural Process in Creep, (1961), 2, ISI, London.
26) M. Yamamoto : Private Communication.
27) T. Yokobori : Zairyo-Kyodo-Gaku, (1967), 139, Gihodo.